Cohesive zone model for intergranular environmental and stress assisted failure and analysis of slow crack growth in ceramic polycrystals

M. Romero de la Osa[1*], R. Estevez[1], C. Olagnon[1], J.Chevalier[1], C.Tallaron[2]
[1] *Université de Lyon, Insa-Lyon, MATEIS CNRS UMR 5510, France;*
[2] *CEA Le Ripault, Monts, France*

Ceramic polycrystals are prone to environmentally assisted Slow Crack Growth (SCG), similarly to vitreous glasses. The kinetics of fracture is known to be dependent on the load level, the temperature and also on the Relative Humidity (RH). In addition, there are evidences that the microstructure influences SCG with an increase in the crack velocity when varying the grain size. This latter observation motivates a local description of fracture with a cohesive zone model for the intergranular failure process. A rate and temperature dependent formulation is proposed to mimic the reaction-rupture mechanism underlying failure. We indicate how the parameters involved in the description can be determined from experiments. We present 2D simulations of intergranular fracture and study the influence of a strong junction or the presence of pores or poor cohesion properties at the triple connection of grains on SCG.

1. Introduction

Polycrystalline ceramics are used in various applications because of their intrinsic advantages such as wear resistance and chemical inertness. Examples are the use of alumina and zirconia for biomedical implants. However, oxide ceramics are prone to a delayed damage mechanism often referred as *slow crack growth* (SCG), which is one of their major drawbacks for demanding, long term applications. This damage process concerns pre-cracked specimens subjected to a mechanical loading in terms of stress intensity factor K_I. It is experimentally shown [1] that, beyond a critical value, crack propagates at a velocity V that increases continuously with rising K_I. SCG has evidenced to be, in addition to time and loading, sensible to environmental conditions (water concentration), temperature and material microstructure [2, 3, 4]. This paper presents a physically motivated cohesive zone model for the description of the reaction-rupture mechanism that underlies failure in ceramics, in particular the intergranular failure mode. From the analysis of failure in a sapphire single crystal, simulations are performed in a 2D polycrystal. We first point out the major role of the triple junction in the resistance to crack propagation. We then investigate the influence of possible defect originating from the sintering process in the form of pores or poorly cohesive triple junction on the crack growth, thus performing some virtual testing to assess if those issues are relevant in the slow crack growth regime and discuss the benefit or losses related to their presence.

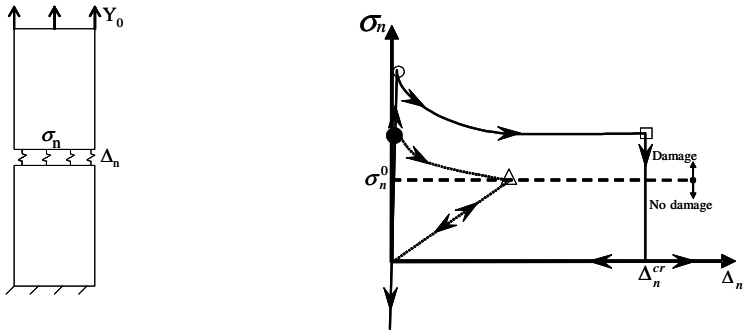

Fig. 1 Schematic description of the cohesive model for the reaction-rupture process under relaxation. The cohesive surfaces are inserted in between two elastic blocks and an overall displacement Y_0 is prescribed.

2. A Cohesive zone model for the reaction-rupture in ceramics

We have recently proposed [5] a cohesive zone model for the reaction-rupture underlying SCG in ceramics. A cohesive zone methodology provides a local description of the failure process and also incorporates a length scale into the analysis. The formulation is briefly reported here, the reader is referred to [5] for further details. A description of the reaction-rupture mechanism has been proposed by Michalske and Freiman [6] in a seminal paper that has received agreement from the ceramic community. More recently, Zhu et al. [7] have revisited and detailed this failure process in ab-initio analyses. Albeit a full multi-scale description in which ab-initio to molecular and eventually continuum frameworks would be connected, we here propose a cohesive surface model inspired by those contributions.

A rate and temperature dependent description is adopted to mimic the chemical reaction-rupture process underlying failure proposed by Michalske and Freiman [6] and inspired by the kinetic fracture observations of Zhurkov [8] and the recent ab-initio calculations of Zhu et al. [7] as [5]

$$\dot{\Delta}_n^c = \dot{\Delta}_0 \exp\left\{\frac{-U_0 + \beta\sigma_n}{k_B T}\right\}$$

in which U_0 represents the energy necessary to break a bond in the absence of any external load. The parameter β corresponds to an activation volume and σ_n represents the traction normal to the interface or grain boundary under consideration. At the denominator, k_B is the Boltzmann constant and T the absolute temperature. The pre-exponential $\dot{\Delta}_0$ term has the dimension of a velocity. Thus, the damage rate $\dot{\Delta}_n^c$ continues until the cumulated $\Delta_n^c = \int \dot{\Delta}_n^c dt$ reaches a critical thickness Δ^{cr}, that correspond to the cease of the mechanical interaction between two separated surface and related nucleation of a crack. The term Δ^{cr} is a material parameter that is thought to be about 1nm in a crystalline material, a distance over which two surfaces do not interact any longer. In this formulation, the influence of the environment can be incorporated through a

dependence of the activation energy U_0 with the aggressive agent, the water in the present case. This case will not be considered in the study, however.
The formulation of the cohesive model is completed with the traction separation

$$\dot{\sigma}_n = k_n \left(\dot{\Delta}_n - \dot{\Delta}_n^c \right),$$

In which $\dot{\Delta}_n$ is the displacement rate prescribed on the cohesive surface and k_n a stiffness 'infinitely' large to ensure $\dot{\Delta}_n \approx \dot{\Delta}_n^c$ during the reaction-rupture process. In Fig. 1, we have reported the response on the foregoing cohesive model inserted in between two elastic blocks under a relaxation test for an initial displacement Y_0. The reaction-rupture process is activated when locally the normal stress on the cohesive surfaces exceeds a threshold value σ_n^0. Depending on the initial value for Y_0, the condition for failure $\Delta_n^c = \int \dot{\Delta}_n^c dt = \Delta_n^{cr}$ is attained and a crack is nucleated locally. When this is not attained but the threshold is recovered prior to this condition, a cumulated damage $\Delta_n^c = \int \dot{\Delta}_n^c dt$ is recorded but the subsequent cohesive response is elastic.
It is worth noting that the damage rate $\dot{\Delta}_n^c$ involved three material parameters ($U_0, \dot{\Delta}_0$ and β). Some insight about U_0 is found in Zhurkhov's analysis who noticed that the activation energy matches with the sublimation energy. In the case of ceramics, this corresponds to 160kJ/mol [8] which we take as a material's data. Therefore, it suffices to calibrate the couple ($\dot{\Delta}_0$ and β) with appropriate experiments to derive a realistically based set of parameters for the cohesive model. This is exemplified in the next section for a sapphire single crystal.

3. Calibration for slow crack growth in sapphire single crystal

We borrowed data from the slow crack growth experiments performed in sapphire single crystal by Salem [9], who investigated slow crack growth under ambient conditions. The corresponding data are reported in Fig. 2 in the form of the slow crack velocity V with the applied load in terms of K_I. We observed that the magnitude of log(V) increases almost linearly with the prescribed K_I. Similarly to [5], we analyse a mode I fracture process under plane strain conditions. Small scale yielding is assumed and a boundary layer approach is adopted that results in prescribing the displacement K_I-fields along the outer boundary (see Fig. 2). A natural crack is considered with a traction free loading along the crack face. Along the crack symmetry plane, where the major principle stress is maximum, cohesive surfaces are inserted, in between two elastic isotropic, linear elastic bulks. Their properties are standard for ceramics with E=390GPa and ν=0.3. The governing equations are based on a rate form of the virtual work

$$\int_v \tau.\delta\dot{\eta}\, dv + \int_{Scz} \sigma_n.\delta\dot{\Delta}_n\, dS = \int_{\partial v} \mathrm{T}.\delta v dS\,,$$

Where τ denotes the second Piola-Kirchhoff stress tensor, η the Lagrangian strain tensor, T the prescribed traction along the outer boundary and v the displacement rate.

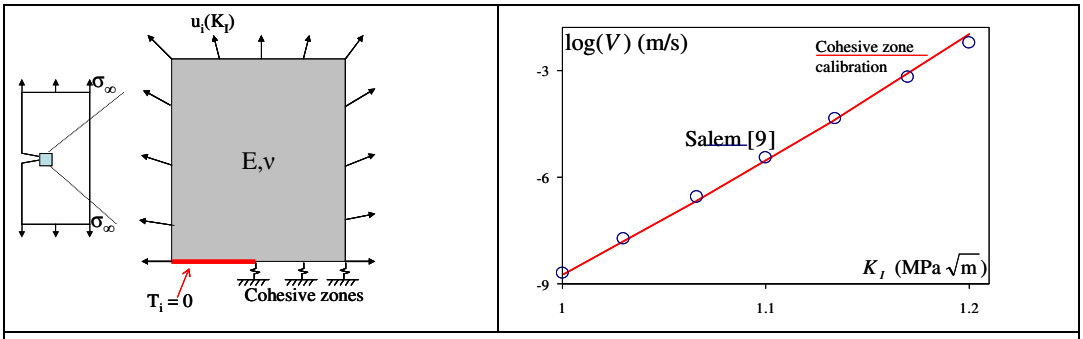

Fig. 2 schematic description of the boundary conditions for the mode I, small scale yielding analysis. Cohesive elements are laid along the crack symmetry plane. The cohesive parameters are calibrated to capture Salem's data [9] for slow crack growth.

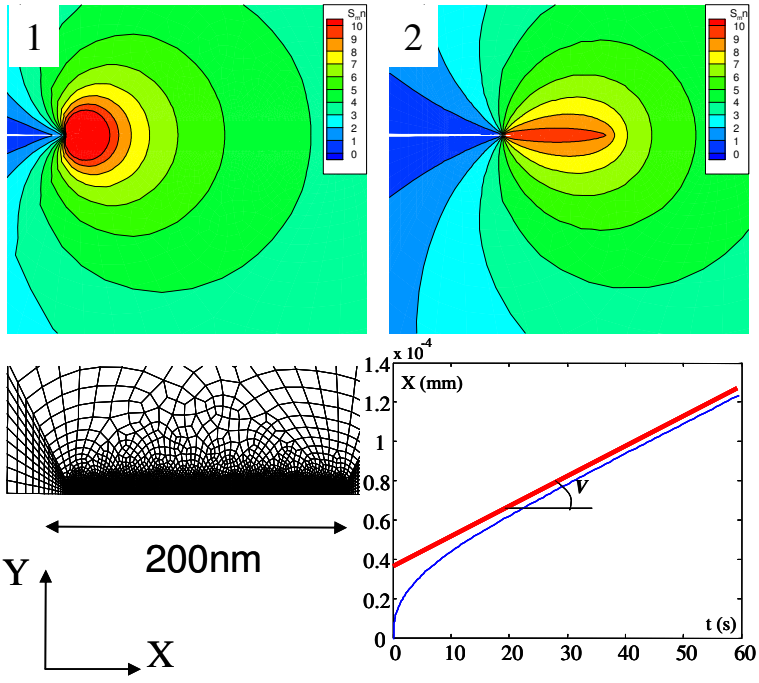

Fig. 3. Mean stress distribution during crack propagation in a single sapphire (GPa), mesh refinement, crack advance versus time and related estimation of the crack velocity.

The contribution of the cohesive surfaces to the virtual work is incorporated in the left hand side. Numerical details on the implementation and variables update are found in [10, 11].

The loading consists in a rapid increase up to the target level K_I during which we have verified that no noticeable damage from the cohesive elements takes place. The load level K_I is then kept constant in time and the cohesive zones accommodate the prescribed loading by relaxing at the damage rate $\dot{\Delta}_n^c$ up to the

opening Δ^{cr} for which a crack nucleates locally. In Fig. 3, we have reported the mean stress contours for two stages during the crack propagation, for a given load level K_I (together with the mesh used for the calculations). The stress concentration indicates the position of the crack tip which is observed to advance during the failure by relaxation.
During a simulation, the crack tip position X with time is recorded and reported as X(t) in Fig. 3. The origin of time corresponds to the onset of crack propagation.
The initiation of crack growth has a transient variation, followed by a steady state crack advance with a linear variation of the crack front X with time. For this steady state regime, we use the tangential slope in X(t) to estimate the crack velocity for the prescribed K_I and derive one prediction in the V(K) diagram of Fig. 2. Repeating this procedure allows us to adjust ($\dot{\Delta}_0$ and β) to capture Salem's experimental data. Starting with the physically realistic values for $\Delta_n^{cr} = 1\text{nm}$ and U_0=160kJ/mol, we have identified $\dot{\Delta}_0 = 3.9\times10^3\text{m/s}$ and $\beta = 0.065\text{nm}^3$.

4. Virtual testing of slow crack growth in ceramic polycrystals

We now consider a small scale damage configuration with a crystalline process zone around the crack tip as depicted in Fig. 4. The overall boundary conditions are the same but the crack path runs along the grain boundaries, the grains are taken isotropic linear elastic for sake of simplicity. Cohesive zones are inserted along the grain boundaries and we use the cohesive parameters identified in the foregoing section. Albeit these have been calibrated for slow crack growth by cleavage in sapphire, we assume that the kinetic of slow crack growth along grain boundaries are similar, cleavage being seen as a 'perfect' grain boundary.
By applying a load level up to a target value K_I that is then maintained constant, we have reported in Fig. 4 the contours plots of the stress component σ_{yy} for different stages of the crack advance. While the initial loading is symmetric and also the crystalline process zone, crack first propagates along an horizontal grain boundary up to the first triple junction. Albeit a similar crack advance is observed along the two oblique grain boundaries, one of them first breaks down thus inducing further propagation towards the negative ordinate Y. In Fig. 4, the stress concentration indicates the current position of the crack tip. This latter is recorded with time and plotted in an X(t) diagram.
We observe that the crack propagation is highly discontinuous in time and exhibits three phases. In a first one corresponding to the propagation of the crack along horizontal grains, X(t) appears almost vertical. A slight reduction in the X(t) slope is observed during the propagation along the oblique grain boundaries. Then, a long incubation time is observed for the transition of the crack path from the oblique towards the horizontal grain facets. The plot X(t) is used to define an average crack velocity for a given load level. This velocity is governed by the slowest part of the propagation history, here corresponding to the transition from oblique to horizontal.

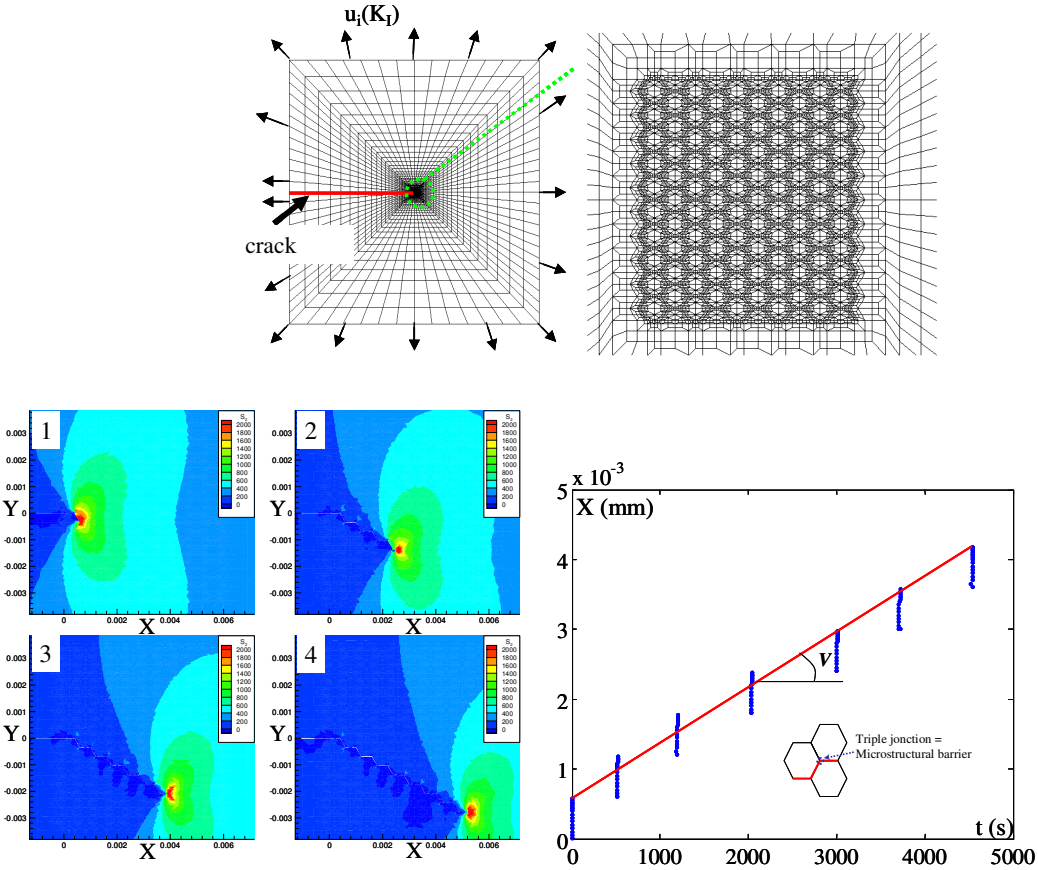

Fig. 4.Problem formulation for slow crack growth in a 2D polycrystal, contour plot of the stress component σ_{yy} (MPa) during the crack propagation, and record of the abscissa of the crack tip with time.

When the crack tip along the oblique facet approaches the triple junction, a crack nucleates ahead on the horizontal grain thus resulting in the creation of an elastic ligament that relaxes the stress. This causes a marked increase in the time $t_R = \Delta_n^{cr} / \dot{\Delta}_n^c$ necessary for a crack to nucleate locally and correspond to the large incubation time observed in X(t) of Fig. 4. At this point, it is worth comparing the slow crack growth predictions between the single crystal and this simple 2D polycrystal.

This is reported in Fig. 4 where we observe a noticeable difference in the crack growth resistance between the single- and poly-crystals predictions. For a given value of the slow crack velocity *V*, the corresponding load is increased by a factor about two. The origin of this shift in the V(K) diagram is not related to an influence of the crack meandering which corresponds to a modest extension of the effective crack length about 2/1.5 increase in the crack path along the grain boundary. The origin of such a reinforcement originates in the dependence of the reaction-rupture $\dot{\Delta}_n^c$ with the local traction σ_n exponentially so that any reduction in the normal stress causes a variation in the local time to rupture of several decades. In the present study and with the parameters we used, this result in a

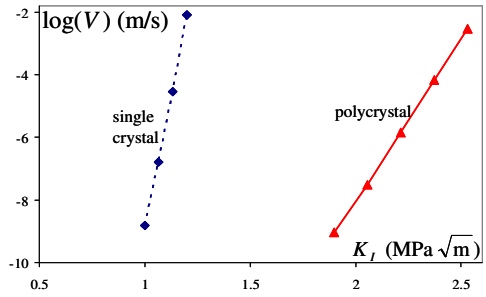

Fig. 5 slow crack growth $V(K_I)$ for a single crystal and a polycrystal.

major slow down of the crack advance at the triple junctions corresponding to the transitions from oblique to horizontal facets. Thus one can consider that these triple junction act as micromechanical obstacles or barriers and appear as the major contribution to the crack growth resistance.

5. Influence of defects originating from the sintering

The above analysis has shown the strong influence of the variations of the local normal stress σ_n on the crack propagation with time with a major influence of the triple junction of the crack growth, at least with the cohesive parameters used here. For the moment, we have assumed perfect triple junctions. These are largely dependent on the quality of the sintering, however, and imperfect triple junctions are observed in some ceramics. The influence of the presence of pores or poor cohesive properties at the triple junctions on slow crack growth is now considered. The initial process zone with pores or precracked surfaces near the triple junctions is depicted in Fig.6. By applying a constant load and observing the crack propagation with time, we have observed a discontinuous crack growth in time with a governing incubation time corresponding in the present cases to the transition from horizontal to oblique grain facet. By estimating the slow crack velocity similarly as in Fig. 4, we report in Fig. 6 the prediction V(K) for the polycrystal with prefect triple junctions and the two other with defects. In Fig.6, we observe that the presence of pores results in an increase of the resistance to slow crack growth with a shift of the V(K) plot towards larger values of the load K for the same crack velocity. On the contrary, the triple junction with poor cohesion properties, and in this case with initial cracks, results in a reduction of the resistance of the slow crack growth with a translation of the V(K) plot towards smaller values of K. The influence of the pores versus 'natural' stress free surfaces in the V(K) predictions originates in the local variations in the normal stress and related local time to rupture t_R. In the case of pores, the stress is less concentrated around the triple junctions thus reducing the crack growth kinetics. In the case of precracks, the faster phases in the crack propagation along the horizontal and oblique grain facets are not arrested near the triple junctions thus resulting is a faster crack velocity at a given load level.

6. Conclusion

We have presented a physically motivated cohesive model to mimic the reaction-rupture mechanism in ceramics. The formulation is able to capture slow crack

growth in single crystal as well as in polycrystals. The cohesive parameters are physically realistic and a comparison with slow crack growth data allows their identification. These have been used for the analysis of slow crack growth in a 2D polycrystal were local variation in the stress acting on the cohesive surfaces are of major importance of the related slow crack growth prediction. The viscoplastic cohesive model used here predicted an increase in the resistance to slow crack growth of polycrystal with respect to single crystals in the order of magnitude found experimentally. The study points out the importance of the local stress fields and their fluctuation of the slow crack growth predictions.

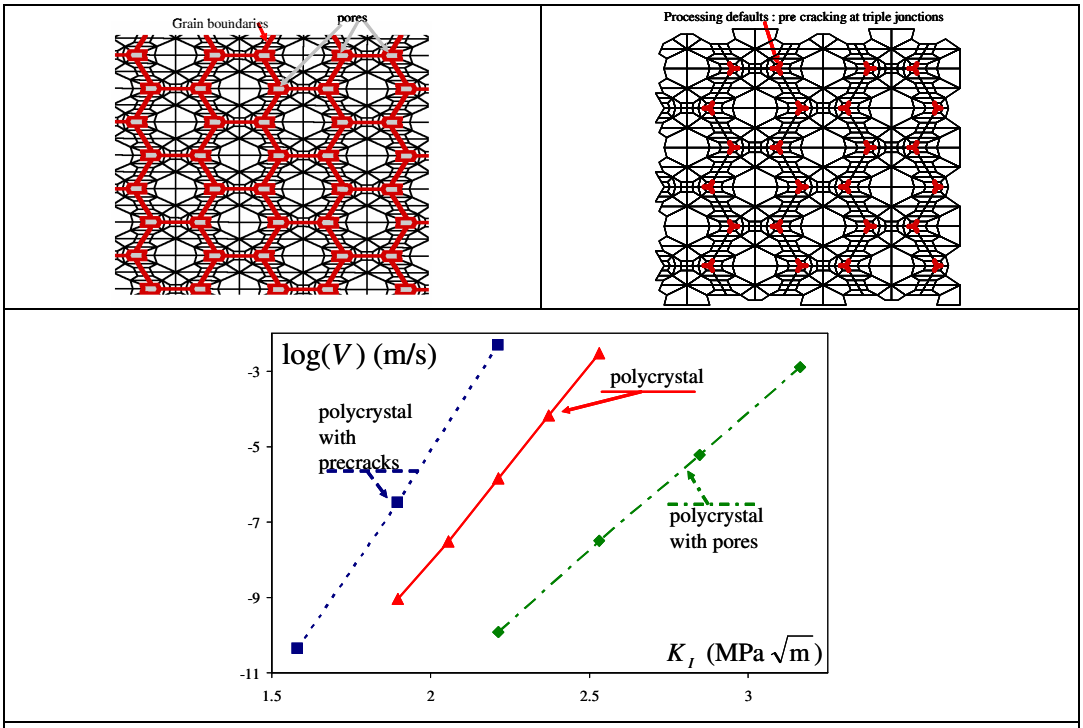

Fig. 6. Process zone with pores or precracks at the triple junctions. Predictions of the slow crack growth $V(K_I)$ for different triple junctions.

References

[1] Wan K. T., Lathabai S., Lawn B. R., J. Eur. Ceram. Soc., 6(1990): 259-268

[2] Wiederhorn S. M., Bolz L. H., J. Am. Cer. Soc. 53(1973) 543-548

[3] Chevalier J., Olagnon, C., Fantozzi G. J. Am. Ceram. Soc., 82 (1999) 3129-3138

[4] Olagnon C., Chevalier J., Pauchard V., J. Eur. Ceram. Soc., 26(2006) 3051-3059

[5] Romero de la Osa, M., Estevez, R., Olagnon, C., Chevalier, J., Tallaron, C. , Vignoud, L., J. Mech. Adv. Mat. Struct., to be published

[6] Michalske, T.A., Freiman, S.W., J. Am. Ceram. Soc. 66 (4) (1983) 284-288

[7] Zhu, T., Li, J., Lin, X., Yip, S., J. Mech. Phys. Solids 53 (2005) 1597-1623

[8] Zhurkov, S.N., J. Fract. Mech. 1 (1965) 311-323

[9] Salem, J.A., NASA/TM—2006-214023

[10] Tijssens M.G.A., Sluys L.J., Van der Giessen, E., Mech. Mat., (2000), 19-35